Resource Allocation in Short Packets BIC-UFMC Transmission for Internet of Things

P. Del Fiorentino, C. Vitiello, V. Lottici,
F. Giannetti and M. Luise
Department of Information Engineering
University of Pisa, Italy

E. Debels. J. Van Hecke and M. Moeneclaey
Department of Telecommunications
and Information Processing (TELIN)
University of Ghent, Belgium

***Abstract*—This paper presents a resource allocation (RA) strategy for bit interleaved coded UFMC (BIC-UFMC) communications to be applied in an Internet of Things scenario characterized by short packets. The proposed RA strategy selects the best transmission parameters (TPs), i.e. code rate, bit loading (BL), power allocation (PA) and number of multicarrier symbols, by maximizing the goodput (GP) metric, defined as the number of correctly received information bits per unit of time, over a frequency-selective fading channel. The results are twofold: *i*) the GP performance of the BIC-UFMC system is further boosted by the best choice of the TPs compared to the case of Uniform PA and BL and a previous GP-based RA solution, named Classical RA; *ii*) considering the frequency offset, the combination of RA and BIC-UFMC reveals to be more robust, i.e. providing higher bit/s/Hz, than the Uniform and Classical cases.**

I. Introduction

Internet of Things (IoT) is playing a crucial role in the fifth generation (5G) mobile network, changing the paradigm of communications from human-to-human to machine-to-machine (M2M). Consequently, IoT requirements are extremely various, depending on the nature of the IoT sensors and on the specific application. However, IoT entities have at least one common feature represented by the small amount of exchanged data, so we can suppose IoT communications can be characterized as a sporadic short-packet transmissions [1]. Furthermore synchronization procedure can be coarse, allowing energy savings at the expense of small time and frequency misalignments. The traditional Orthogonal Frequency Division Multiplexing (OFDM) waveform developed for the fourth generation (4G) networks may not be suitable for the IoT features mentioned above. Indeed, OFDM exploits a strict synchronization procedure to preserve orthogonality, which causes high signalling overhead, which is in contrast with sporadic and short packets communication. In the light of the above, new 5G waveforms, falling within the category of non-orthogonal and asynchronous modulations, have been proposed to overcome the limitation of synchronism and orthogonality required by the 4G physical layer. For example, Filter Bank Multicarrier (FBMC) [2] provides per-subcarrier filtering, increasing robustness against the effects of misalignment, but time efficiency, defined as the ratio between information carried by the multicarrier symbol and its overall length, decreases due to the long filter length required for having narrow filtering. Another important 5G waveform is the Generalized Frequency Division Multiplexing (GFDM) [3], which is based on per-subcarrier circular filtering of a block of symbols. Universal Filtered Multicarrier (UFMC) comes out as a tradeoff between OFDM and FBMC [4]. UFMC processing groups subcarriers into subbands, on which IFFT and filtering are performed. UFMC increases robustness against time and frequency offset, improving the spectral efficiency and reducing out-of-band emissions without losing OFDM advantages [5]. In parallel with the study of novel waveforms, the efficient resource allocation (RA) of the transmission parameters (TPs) comes out as one of the main challenges to be met in the 5G physical layer wireless communications [1].

In this paper, we present a RA strategy for a bit interleaved coded UFMC (BIC-UFMC) system for short packets communications over a frequency-selective fading channel, assuming perfect knowledge of channel state information (CSI). We also include the BIC modulation, in order to improve the systems performance as shown in [6]. The proposed scenario is far from the typical IoT one because we choose to focus on the RA of a single IoT entity in order to maximize its performance before to extend the results to a more complex scenario. Given that the proposed waveform can easily coexist with the 4G OFDM [5], in our paper, IoT sensor can use a LTE-like version of UFMC for communicating with a UFMC eNB exploiting the mobile network infrastructure. The presented RA solution chooses the best TPs by maximizing the goodput (GP) metric, defined as the number of correctly received information bits per unit of time [7]. The GP metric is exploited because it is a suitable solution to evaluate the performance of packet-oriented systems. In the previous work [8][9], the RA strategy was based on the optimization of the TPs, i.e. code rate, bit loading (BL) vector, representing the number of bits loaded over the subcarriers and power allocation (PA) vector. Here instead, we further include the number of multicarrier symbols to transmit a packet. In detail, we adapted the strategies proposed in [10] and [11], by modifying the RA problem, in order to maximize the reliability over the IoT link, where very short packets are transmitted. Numerical results confirm that the presented RA strategy is an excellent method to allocate the TPs with respect to the original PA and BL methods and the uniform BL and PA case. Finally, the robustness of the presented RA in the presence of frequency offset was evaluated and compared to the GP performance of conventional BIC-

OFDM transmission.

Notations. Vectors are in in bold, $[\cdot]^{\mathrm{T}}$ is the transpose operator, $\lfloor x \rfloor$ is the lower integer of x, $\{x\}^a \triangleq \max\{a, x\}$ and $\mathbb{N}$ is the set of natural numbers.

II. System Model

The classical IoT scenario is composed by hundreds of entities which want to communicate at the same time. Here, we concentrate our efforts on just one of this entities, assuming an uplink LTE-like communication and focusing on its resource allocation strategy for improving the communication performance. The BIC-UFMC system receives packets from a data link layer, with a packet length of N_{u} bits, which are divided in N_{p} bits of payload and N_{CRC} bits of cyclic redundancy check (CRC). The BIC block encodes the N_{u} bits, with a code rate $r \in \mathcal{D}_{\mathrm{r}} \triangleq \{r_0, \cdots, r_{|\mathcal{D}_r|}\}$, and interleaves the bits. Subsequently, the sequence of interleaved and coded bits is processed by the UFMC modulator, shown in Fig. 1, which will transmit the bits from one packet by means of U multicarrier symbols. In order to simplify the description of the system model, we illustrate the UFMC signal processing, considering a single multicarrier symbol. In detail, the bits are loaded over N subcarriers, according to the BL vector $\mathbf{m} \triangleq [m_0, \cdots, m_{N-1}]^{\mathrm{T}}$, whose generic element $m_n \in \mathcal{D}_m \triangleq \{0, \cdots, m_{\max}\}$ represents the number of bits on the n-th subcarrier, from 0 to $m_{\max}$. The loaded bits are Gray-mapped to complex symbols, employing the unit-energy constellation $\chi_n \triangleq 2^{m_n}$-QAM, $\forall n \in \mathcal{N} \triangleq \{0, \cdots, N-1\}$, obtaining the vector $\mathbf{s} \triangleq [s_0, \cdots, s_{N-1}]^{\mathrm{T}}$. The vector $\mathbf{s}$ is element-wise multiplied by the square root of the PA vector $\mathbf{p} \triangleq [p_0, \cdots, p_{N-1}]^{\mathrm{T}}$ satisfying the condition that $\sum_{n=0}^{N-1} p_n \leq P_{\mathrm{tot}}$, where P_{tot} is the available power. The resulting vector $\mathbf{X} \triangleq [X_0, \cdots, X_{N-1}]^{\mathrm{T}}$, with $X_n \triangleq \sqrt{p_n} s_n$, is split over B subbands, each composed of D subcarriers, so that $N = BD$. The partition of $\mathbf{X}$ for the generic subband $i \in \mathcal{B} \triangleq \{0, \cdots, B-1\}$ is defined as $\mathbf{X}_i \triangleq [X_{iD}, \cdots, X_{iD+D-1}]^{\mathrm{T}}$. In each subband an IFFT, with size N_{FFT}, of $\mathbf{X}_i$ is performed, obtaining the time-domain vector $\mathbf{x}_i$. The vector $\mathbf{x}_i$ is then filtered by a Dolph-Chebyshev finite impulse response (FIR) filter $\mathbf{q}_i \triangleq [q_{i,0}, \cdots, q_{i,L-1}]^{\mathrm{T}}$, with 60 dB of side lobe attenuation and length L, tuned to the i-th subband by a normalized frequency shift $\omega_i \triangleq \frac{D-1}{2} + iD$, $\forall i \in \mathcal{B}$. At the output of each filter, the generic u-th element $z_{i,u}$ is given by

$$z_{i,u} \triangleq \sum_{m=0}^{N_{\mathrm{FFT}}-1} x_{i,m} q_{i,u-m}. \tag{1}$$

The vectors $\mathbf{z}_i \triangleq [z_{i,0}, \cdots, z_{i,N_{\mathrm{FFT}}+L-1}]^{\mathrm{T}}$ from all subbands are element-wise summed and finally the resulting multicarrier symbol $\mathbf{z} \triangleq \sum_{i=0}^{B-1} \mathbf{z}_i$ is sent over a frequency-selective fading channel; the channel impulse response (CIR) $\mathbf{h}$ is assumed stationary for the whole transmission of a packet. Considering only one multicarrier symbol, the received signal in the time-domain turns out to be

$$r_l \triangleq \sum_{m=0}^{N_{\mathrm{FFT}}+L-1} z_m h_{l-m} + w_l, \tag{2}$$

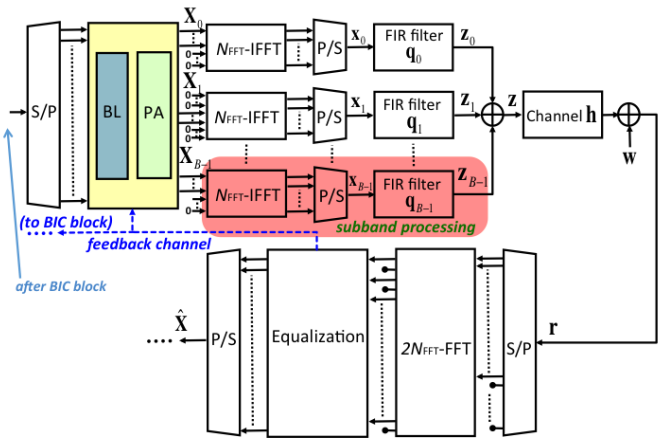

Fig. 1. UFMC architecture

where $l = 0, \cdots, N_{\mathrm{FFT}}+L+L_{\mathrm{CH}}-3$, L_{CH} is the length of the channel impulse response and $w(l) \in \mathcal{CN}(0, \sigma^2)$ is a sample of complex Gaussian noise. The first $N_{\mathrm{FFT}} + L - 1$ samples of the received signal (2) are zero-padded and processed by an FFT of size $2N_{\mathrm{FFT}}$. The resulting samples are down-sampled by factor 2, taking only the even-indexed subcarriers [4]. So the frequency-domain sample corresponding to the subcarrier k is

$$Y_k \triangleq H_k \sum_{i=0}^{B-1} Q_{i,k} \tilde{X}_{i,k} + \mathcal{I}_k + W_k, \tag{3}$$

where $k = 0, 2, \cdots, 2N_{\mathrm{FFT}}-2$, H_k, $Q_{i,k}$, $\tilde{X}_{i,k}$ and W_k represent the generic k-th element of the $2N_{\mathrm{FFT}}$-FFT output related to the CIR $\mathbf{h}$, FIR filter $\mathbf{q}_i$, symbols $\mathbf{x}_i$ and ambient noise respectively. Furthermore, $\mathcal{I}_k$ is the interference contribution analyzed in [12], which includes the intercarrier interference (ICI) due to the FFT processing of only $N_{\mathrm{FFT}}+L-1$ samples from (2), the intersymbol interference (ISI) as a result of the overlapping of consecutive multicarrier symbols and also an amplitude reduction factor of the useful signal due to the non-orthogonality. Given that a $2N_{\mathrm{FFT}}$-FFT is used, $\tilde{X}_{i,k}$ can be written as

$$\tilde{X}_{i,k} = X_{\frac{k}{2}} = \sqrt{p_{\frac{k}{2}}} s_{\frac{k}{2}}, \quad \text{for } \frac{k}{2} = iD, \cdots, iD + D - 1. \tag{4}$$

Therefore, eq. (3) becomes

$$Y_n \triangleq H_n Q_{i(n),n} \sqrt{p_n} s_n + \mathcal{I}_n + W_n, \tag{5}$$

with $n \in \mathcal{N}$ and $i(n) \triangleq \lfloor n/D \rfloor$, $i(n) \in \mathcal{B}$. After the UFMC receiver processing, the signal (5) is equalized by a zero forcing (ZF) equalizer and is soft-decoded.

III. Goodput Performance Metric

The GP is an useful metric for providing reliable information about the link performance when modulation and coding schemes are employed. The actual GP performance value can be estimated by means of a function called expected GP (EGP)

[11], which is the objective function of the RA problem. We approximate the signal (5) as

$$Y_n \cong H_n Q_{i(n),n} \sqrt{p_n} s_n + W_n, \tag{6}$$

by discarding the interfence term $\mathcal{I}_n$. Its effect is attenuated by the subband filtering $\mathbf{q}_i$, $\forall i \in \mathcal{B}$, as shown in [12], making the UFMC signal quasi-orthogonal and allowing to easily exploit the EGP function. Nevertheless, in Sec. V, the interference term $\mathcal{I}_n$ has been evaluated, confirming the validity of the approximation (6). Starting from Eq. (6), the received signal to noise ratio (SNR) vector, normalized by the transmitted power, can be defined as $\mathbf{\Gamma} \triangleq [\gamma_0, \cdots, \gamma_{N-1}]^{\mathrm{T}}$, where its generic element is

$$\gamma_n \triangleq \frac{|H_n|^2 \left|Q_{i(n),n}\right|^2}{\sigma^2}. \tag{7}$$

The EGP can be expressed in bits/s/Hz as [11]

$$\zeta(\phi, U, \mathbf{p}) \triangleq \frac{N_{\mathrm{FFT}}}{N_{\mathrm{FFT}} + L - 1} \frac{N_{\mathrm{p}}}{UN} [1 - \Phi_r(\gamma_{\mathrm{eff}})], \tag{8}$$

with $U \triangleq N_{\mathrm{u}}/r \sum_{n=0}^{N-1} m_n$ the number of multicarrier symbols of a packet, $\phi \triangleq (r, \mathbf{m})$ the transmission mode (TM) and $N_{\mathrm{FFT}}/N_{\mathrm{FFT}} + L - 1$ is a normalization factor for considering the filter length. Moreover, $\Phi_r(\gamma_{\mathrm{eff}})$ represents the packet error rate (PER) of the link, which depends on the *effective* SNR γ_{eff}. The *effective* SNR is calculated by exploiting the κESM link performance prediction (LPP) method and its formula is given by [11]

$$\gamma_{\mathrm{eff}} \triangleq -\log \left[\frac{1}{\sum_{n=0}^{N-1} m_n} \sum_{n=0}^{N-1} \alpha(m_n) \mathrm{e}^{-p_n \gamma_n \beta(m_n)} \right], \tag{9}$$

where $\alpha(m_n)$ and $\beta(m_n)$ are constant values depending only on the size m_n, $\forall n \in \mathcal{N}$, of the QAM constellation.

IV. Resource Allocation Problem and Solution

The purpose of the RA technique is to efficiently calculate the best PA vector $\mathbf{p}^* \triangleq [p_0^*, \cdots, p_{N-1}^*]^{\mathrm{T}}$ and TM $\phi^* \triangleq (r^*, \mathbf{m}^*)$, where $\mathbf{m}^* \triangleq [m_0^*, \cdots, m_{N-1}^*]^{\mathrm{T}}$ is the best BL vector, by maximizing the EGP function (8). Furthermore, unlike previous work [8], the RA strategy selects the best number of multicarrier symbols U^* to transmit the packet. The CSI required to the RA strategy is the SNR vector $\mathbf{\Gamma}$, which is sent from the receiver to the BIC-UFMC transmitter through a feedback channel as depicted in Fig. 1, under the hypothesis of perfect estimation of $\mathbf{\Gamma}$. Therefore, the RA optimization problem (OP) can be introduced as follows

$$\begin{aligned} (\phi^*, \mathbf{p}^*, U^*) = \arg\max_{\phi, \mathbf{p}, U} \{\zeta(\phi, U, \mathbf{p})\} \\ \text{s.t.} \quad \phi \in \Psi \\ \Delta(\mathbf{m}) = \tfrac{C(r)}{U} \\ \sum_{n=0}^{N-1} p_n \leq P_{\mathrm{tot}} \end{aligned}, \tag{10}$$

where $\Psi \triangleq \mathcal{D}_r \times \mathcal{D}_m$ is the set of feasible TMs, $\Delta(\mathbf{m}) \triangleq \sum_{n=0}^{N-1} m_n$ and $C(r) \triangleq N_{\mathrm{u}}/r$ is the number of coded bits for a packet. Allow us to make a brief remark on the constraint $\Delta(\mathbf{m}) = C(r)/U$ in (10). This constraint has been included with the aim of equally dividing the coded bits over the number of UFMC symbols U. In [8] this constraint was not considered, which lead to a bit allocation and code rate that maximize the goodput of a single multicarrier symbol. However by using these TPs, it was very likely that the last multicarrier symbol of a packet was only partially used. The last multicarrier symbol had only a limited influence on the performance in [8], because these scenarios required the transmission of many multicarrier symbols for transmitting a single packet. Instead in this work, we consider short packets that require the transmission of only a few multicarrier symbols. By loading less bits on the different subcarriers or by using a lower code rate, we can fully utilize different UFMC symbols and are thus able to increase the reliability of the system.

We will tackle the joint OP (10), by separating it in the following two subproblems.

1) Given uniform PA (UPA), $p_n = P_{\mathrm{tot}}/N$, $\forall n \in \mathcal{N}$, the best TM ϕ^* and number of UFMC symbols U^* are derived;
2) The best PA vector $\mathbf{p}^*$ is calculated.

A. TM Solution

Given UPA, the TM OP is

$$\begin{aligned} (\phi^*, U^*) = \arg\max_{\phi, U} \{\zeta(\phi, U)\} \\ \text{s.t.} \ \phi \in \Psi \\ \Delta(\mathbf{m}) = \tfrac{C(r)}{U} \end{aligned}. \tag{11}$$

The problem (11) can be solved by means of the *greedy* algorithm from [10] with the aim of reducing the computational complexity to $\mathcal{O}(\mathcal{D}_r N \log N)$ with respect to an exhaustive search of ϕ^* and U^*. In detail, for a given code rate r, the best BL vector is calculated with the *greedy* algorithm for $U = 1, 2, 3, \cdots$. For each U, the algorithm finds a BL vector $\mathbf{m}$, which satisfies the constraint $\Delta(\mathbf{m}) = C(r)/U$. Finally, the value of U, which yields the largest EGP, is selected. The procedure is repeated for each code rate $r \in \mathcal{D}_r$ in order to find the best TM ϕ^* and U^*. By the way, a clarification is needed: the *greedy* algorithm is time consuming and this drawback can limit its utilization only on IoT applications without very low latency requirements.

B. PA Solution

The best PA vector $\mathbf{p}^*$ is found by the following OP

$$\begin{aligned} \mathbf{p}^* = \arg\max_{\mathbf{p}} \{\zeta(\phi^*, U^*, \mathbf{p})\} \\ \text{s.t.} \ \sum_{n=0}^{N-1} p_n \leqslant P_{\mathrm{tot}} \\ p_n \geqslant p_{\min}, \quad \forall n \in \tilde{\mathcal{N}} \end{aligned}, \tag{12}$$

where $\tilde{\mathcal{N}} \triangleq \{\forall n \in \mathcal{N} : m_n \neq 0\}$ and $p_{\min}$ is the minimum allocated power. The $p_{\min}$ value is necessary to avoid that the PA process turns off some subcarriers, thus holding the constraint $\Delta(\mathbf{m}) = C(r)/U$. From the EGP function (8), we see that the EGP maximization over $\mathbf{p}$ is equal to minimize

the numerator of the log function in γ_{eff} (9). Thus, the PA OP becomes

$$\begin{aligned} \mathbf{p}^* &= \arg\min_{\mathbf{p}} \{f(\mathbf{p})\} \\ \text{s.t.} &\sum_{n=0}^{N-1} p_n \leqslant P_{\text{tot}} \\ &p_n \geqslant p_{\min}, \quad \forall n \in \tilde{\mathcal{N}} \end{aligned}, \tag{13}$$

where

$$f(\mathbf{p}) \triangleq \sum_{n=0}^{N-1} \alpha(m_n^*) \mathrm{e}^{-p_n \gamma_n \beta(m_n^*)}. \tag{14}$$

Proposition 1. The OP (14) is convex [13] whose solution, $\forall n \in \tilde{\mathcal{N}}$, is given by

$$p_n^* \triangleq \left\{ \frac{1}{\gamma_n \beta(m_n^*)} \left[\log \frac{1}{\vartheta} - \log \left(\frac{1}{\gamma_n \alpha(m_n^*) \beta(m_n^*)} \right) \right] \right\}^{p_{\min}}. \tag{15}$$

Proof. See Appendix A. ■

The value of $p_{\min}$ is computed only once, before starting the transmission, as

$$\begin{aligned} p_{\min}^* = & \frac{\sum_{i=\text{SNR}_{\min}}^{\text{SNR}_{\max}} \arg\max_{p_{\min}^{(i)}} \{\text{E}_{\mathbf{H}}\{\zeta(\phi, U, \mathbf{p})\}\}}{N_{\text{SNR}}} \\ \text{s.t.} \quad & 0 < p_{\min}^{(i)} \leqslant \frac{P_{\text{tot}}}{N} \end{aligned}, \tag{16}$$

where $\text{E}_{\mathbf{H}}\{\cdot\}$ is the expectation operator with respect to the frequency channel vector $\mathbf{H}$ and N_{SNR} is the steps number of SNR interval. Table I summarizes the RA pseudo-code.

1) **Initialize:** code rate vector $\mathbf{r} = [r_1, \cdots, r_{\max}]^{\text{T}}$, $\zeta_{\text{temp}} = 0$
2) **For** $i = 1 : \text{length}\{\mathbf{r}\}$
3) **Evaluate:** $C(\mathbf{r}[i])$ and $\phi[i] = \underset{\substack{\mathbf{m} \in \mathcal{D}_m \\ \Delta(\mathbf{m}) = C(\mathbf{r}[i])/U}}{\arg\max} \{\zeta(\mathbf{m}, \mathbf{r}[i]), U)\}$, for $U = 1, 2, \cdots$ until $\zeta(\mathbf{m}[i], \mathbf{r}[i]), U+1) < \zeta(\mathbf{m}[i], \mathbf{r}[i]), U)$ where $\phi[i] = (\mathbf{m}[i], \mathbf{r}[i])$;
4) **If** $\zeta(\mathbf{m}[i], \mathbf{r}[i]), U\} > \zeta_{\text{temp}}$
5) **Set:** $\phi^* = \phi[i]$, $U^* = U$, $\zeta_{\text{temp}} = \zeta(\mathbf{m}[i], \mathbf{r}[i]), U\}$;
6) **End If**
7) **End For**
8) **Evaluate:** p_n^*, $\forall n \in \tilde{\mathcal{N}}$, in (15);
9) **Return** ϕ^*, U^* and $\mathbf{p}^*$;

TABLE I
RA PSEUDO-CODE

V. Numerical Results

The usefulness of the proposed RA strategy, which we call *Constrained RA*, is shown for the transmission of short packets. In particular, the Constrained RA is compared to the Classical RA, which uses BL and PA of [8], and also to a lower bound called Uniform RA, which applies uniform PA $p_n^* = P_{\text{tot}}/N$ and uniform BL $m_n^* = m^*$, $\forall n \in \mathcal{N}$. The GP performance is measured by averaging the number of bits/s/Hz correctly received on the total amount of N_{pkt} = 1000 transmitted packets for each SNR value. Thus, the average GP (AGP) is calculated as

$$\bar{\zeta} \triangleq \frac{N_{\text{FFT}}}{N_{\text{FFT}} + L - 1} \frac{N_{\text{p}}}{N N_{\text{u}} N_{\text{pkt}}} \sum_{i=0}^{N_{\text{pkt}}-1} r_i^* \sum_{n=0}^{N-1} m_{i,n}^* \delta(i), \tag{17}$$

where $\delta(i) = 1$ if the i-th packet is correctly decoded and 0 when it is discarded, and r_i^* and $m_{i,n}^*$, $\forall n \in \mathcal{N}$, represent the best TM for the i-th transmitted packet. Table II summarizes the set of simulation parameters, which are referred to the LTE standard with 10MHz channelization [14] and the payload length N_{p} is chosen on the basis of the user datagram protocol (UDP). Moreover, the extended vehicular A (EVA) channel [15] and the modified COST231 Hata path loss (PL) model [16] are implemented, considering independent channel realizations for each transmitted packet. The SNR points are calculated as $\text{SNR} \triangleq P_{\text{tot}}/(P_{\text{noise}}\Theta)$ by varying P_{tot}, with Θ the PL value. A convolutional code is exploited to simplify the soft-decoding, however, a turbo code can be applied as well, by adding an adjusting factor in Eq. (9) [17].

First of all, in order to validate the approximation of the received signal in (6), we measure the interference at the output of the ZF equalizer, evaluating the mean square error (MSE). Thus, calling $\hat{X}_{i,n}$ as the zero-forcing equalized version of $Y_{i,n}$, the MSE is given by

$$\text{MSE} \triangleq \frac{1}{N_{\text{pkt}}} \sum_{i=1}^{N_{\text{pkt}}-1} \sum_{n=0}^{N-1} \frac{|\hat{X}_{i,n} - s_{i,n}|^2}{N}, \tag{18}$$

in absence of ambient noise and fixing the code rate $r = 1/2$. The MSE value due to interference is around -58 dB, therefore the approximation in (6) is justified. This means that the interference on the signal is well attenuated by the presence of the filter $\mathbf{q}$.

After checking the correctness of the signal model required for the RA, the comparison of the Constrained, Classical and Uniform RAs can be shown. Figure 2 clearly depicts the excellent AGP performance of the Constrained RA, obtaining a constant gain compared to the Classical and Uniform strategies, up to the maximum GP calculated as $\text{GP}_{\max} = N_{\text{p}}/N = 1.25$ bits/s/Hz. It is to be emphasized that, the Constrained RA provides a better GP performance than Classical and Uniform algorithms, because the spectral efficiency is maximized. Indeed, the available subcarriers are always used. Instead, the aim of the Classical RA is only to maximize the EGP function, not considering the length of a packet. Therefore, more bits than necessary could be allocated in the BL vector with the Classical strategy and consequently not all the available subcarriers will be exploited. Figure 3, instead, compares EGP and AGP values in order to verify if the EGP function (8) properly estimates the GP link performance. As can be seen, the value of AGP and EGP are quite close. Now, we include in the received signal a frequency offset, which is time-domain formalized for the subband i as [4]

$$c_{i,m} \triangleq \mathrm{e}^{\frac{j2\pi\varepsilon m}{N_{\text{FFT}}}}, \forall i \in \mathcal{B}, \tag{19}$$

where $m = 0, \cdots, N_{\mathrm{FFT}}+L-1$ and ε is the carrier frequency offset (CFO) normalized for the subcarrier spacing. In the first simulation, Constrained, Classical and Uniform RAs are compared to each other. As Fig. 4 depicts, the Constrained RA considerably makes the system more robust. The excellent result is explained by the fact that the BL algorithm loads only the required bits to transmit the packet. Considering that the packet has a short length, few bits are transmitted over all the available subcarriers, being able to select a reduced QAM constellation and a low code rate with the result that the reliability of the transmission is maximized. Finally, the GP performances of the BIC-UFMC and BIC-OFDM systems are compared, using the Constrained RA. In order to ensure a fair comparison, the ambient noise variance for the BIC-OFDM is set to $\sigma^2_{\mathrm{OFDM}} = \sigma^2(N_{\mathrm{FFT}}/N_{\mathrm{FFT}} + L - 1)$, the cyclic prefix is $\mathrm{CP} = L-1$ and the CFO is imposed equal for the whole bandwidth [12]. As expected, Fig. 5 shows that for CFO values around 0, BIC-UFMC and BIC-OFDM systems return the same performance, because the non-orthogonality that characterizes an UFMC signal, which is included in the term $\mathcal{I}_n$, $\forall n \in \mathcal{N}$, is negligible. Instead, by increasing the CFO, the BIC-UFMC can provide better GP performance, because the N subcarriers are divided in subbands, which are filtered, thus the whole interference is attenuated. However, the gap between the two curves in Fig. 5 is not particularly big, demonstrating that the Constrained RA is able also to increase the robustness of a BIC-OFDM transmission.

Simulation Parameters	***Value***
Information bits (N_{p})	150
CRC (N_{CRC})	32
Subcarriers (N)	120
Subbands (B)	10
FFT size	1024
Bandwidth	10 MHz
QAM modulation order (m_n)	2, 4, 6
Convolutional code rate (r)	1/2, 2/3, 3/4, 5/6
Noise power in bandwidth (P_{noise})	-100 dBm
Variance ambient noise (σ^2)	P_{noise}/N
Distance transmitter-receiver	141 m
Minimum power per subcarrier (p^*_{min})	$0.53(P_{\mathrm{tot}}/N)$

TABLE II
SYSTEM PARAMETERS

VI. CONCLUSIONS

We presented a Constrained RA strategy that selects code rate, modulation format, power distribution across subcarriers and the number of multicarrier symbols for transmitting a short packet. From the results, it is clear that: *i*) our solution can further boost GP performance compared to the Classical and Uniform RAs; *ii*) in presence of CFO, a significant gain in terms of robustness is obtained compared to Uniform and Classical RAs and also combining the classic BIC-OFDM with the Constrained RA. Therefore, the imposed constrain $\Delta(\mathbf{m}) = C(r)/U$ was confirmed to be an optimal modification to adapt the Classical RA for a possible IoT scenario characterized by short packets.

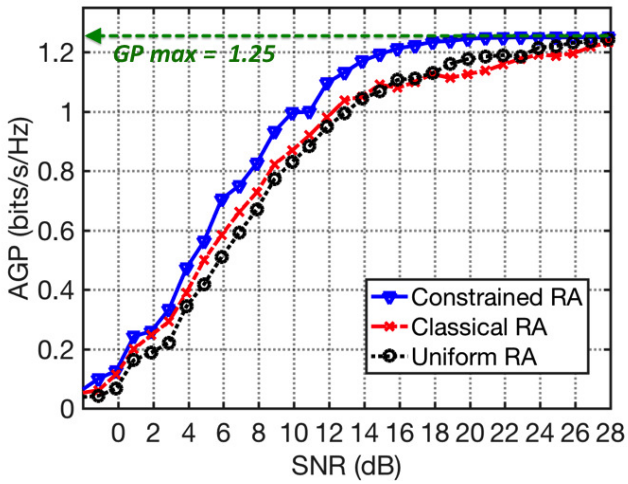

Fig. 2. Comparison of the RA strategies

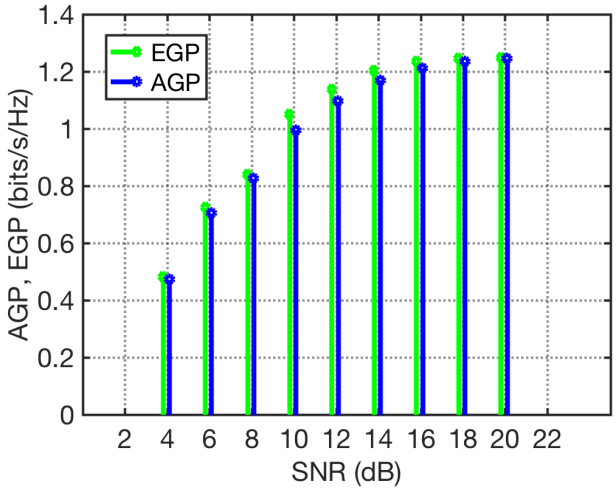

Fig. 3. EGP vs AGP

APPENDIX A

From the convex OP (14), the Lagrangian is written as

$$\mathcal{L}(p^*_0, \cdots, p^*_{N-1}, \lambda_0, \cdots, \lambda_{N-1}, \vartheta) \triangleq$$
$$\triangleq \sum_{n=0}^{N-1} \alpha(m^*_n) \mathrm{e}^{-p^*_n \gamma_n \beta(m^*_n)} - \sum_{n=0}^{N-1} \lambda_n (p^*_n - p_{\mathrm{min}}) +$$
$$+ \vartheta \left(\sum_{n=0}^{N-1} p^*_n - P_{\mathrm{tot}} \right), \qquad (20)$$

where $\lambda_0, \cdots, \lambda_{N-1}, \vartheta$ are the Lagrange multipliers. By applying the Karush-Kuhn-Tucker (KKT) conditions [13], the following equations are obtained:

$$\frac{\partial \mathcal{L}}{\partial p^*_n} \triangleq -\alpha(m^*_n)\gamma_n \beta(m^*_n) \mathrm{e}^{-p^*_n \gamma_n \beta(m^*_n)} - \lambda_n + \vartheta = 0, \quad (21)$$

$$p^*_n \geqslant p_{\mathrm{min}}, \qquad (22)$$

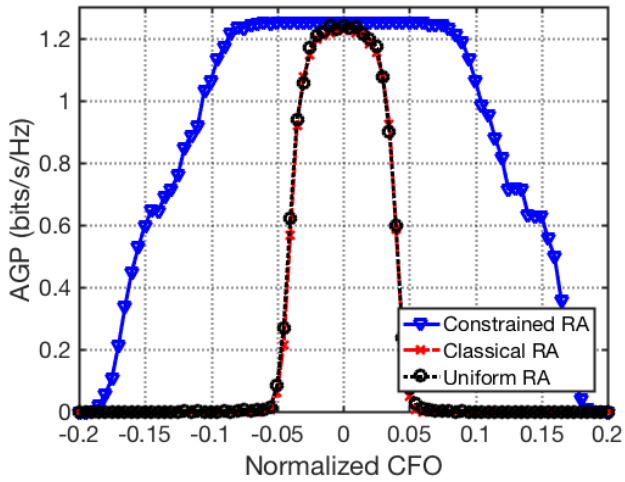

Fig. 4. Comparison of the RA strategies (SNR = 28 dB)

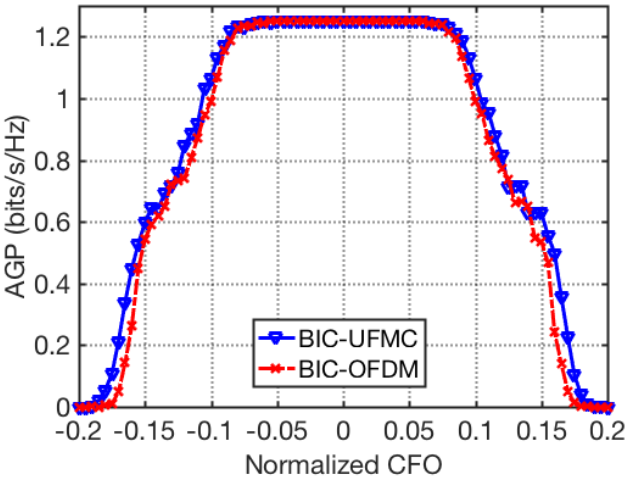

Fig. 5. BIC-UFMC vs. BIC-OFDM with Constrained RA (SNR = 28 dB)

$$\sum_{n=0}^{N-1} p_n^* \leq P_{\text{tot}}, \tag{23}$$

$$\lambda_n \geqslant 0, \tag{24}$$

$$\lambda_n (p_n^* - p_{\min}) = 0. \tag{25}$$

Thus, from Eq. (21), λ_n is calculated, which is replaced in (25) in order to obtain the optimal power p_n^* (15), $\forall n \in \tilde{\mathcal{N}}$, according to (22) and (24). The solution (15) represents the typical water-filling solution [13], where $\log(1/\vartheta)$ is the water level evaluated so that $\sum_{n=0}^{N-1} p_n^* = P_{\text{tot}}$.

Acknowledgment: The work is supported by the PRA 2016 research project 5GIOTTO funded by the University of Pisa.

REFERENCES

[1] Wunder, G.; et al., "5GNOW: non-orthogonal, asynchronous waveforms for future mobile applications", in Comm., *IEEE Magazine on* , 2014.

[2] Farhang-Boroujeny, B.,"OFDM Versus Filter Bank Multicarrier," in Signal Process., *IEEE Magazine on*, vol. 28, no. 3, pp. 92-112, May 2011.

[3] Michailow, N.; et al., "Generalized Frequency Division Multiplexing for 5th Generation Cellular Networks," in Comm., *IEEE Trans. on*, 2014.

[4] Wang, X.; Wild, T.; Schaich, F.; et al., "Universal Filtered Multi-Carrier with Leakage-Based Filter Optimization", *European Wireless Conf.*, 2014.

[5] Kaltenberger, F.; Knopp, R,; Vitiello, C; Danneberg, M; and Festag, A., "Experimental analysis of 5G candidate waveforms and their coexistence with 4G systems", JNCW 2015, http://www.eurecom.fr/publication/4725

[6] Caire, G.; Taricco, G.; Biglieri, E., "Bit-interleaved coded modulation," in Inform. Theory, *IEEE Trans. on* , vol.44, no.3, pp.927-946, May 1998.

[7] Qiao, D.; et al., "Goodput analysis and link adaptation for IEEE 802.11a wireless LANs", Mobile Computing, *IEEE Trans. on* , 2002.

[8] Del Fiorentino, P.; Vitiello, C; Lottici, V.; Giannetti F.; Luise, M., "A Robust Resource Allocation Algorithm for Packet BIC-UFMC 5G Wireless Communications", *EUSIPCO 2016*, August 2016.

[9] Vitiello, C; Del Fiorentino, P.; Debels, E.; Lottici, V.; Giannetti F.; Luise, M.; Moeneclaey M., "Two-Step Resource Allocation for BIC-UFMC Wireless Communication", *2016 International Symposium on Wireless Communication Systems (ISWCS)*, Sept. 2016.

[10] Stupia, I.; Giannetti, F.; Lottici, V.; Vandendorpe, L., "A greedy algorithm for goodput-based adaptive modulation and coding in BIC-OFDM systems," *European Wireless Conf.*, 2010, pp. 608-615.

[11] Stupia, I.; Lottici, V.; Giannetti, F.; Vandendorpe, L., "Link Resource Adaptation for Multiantenna Bit-Interleaved Coded Multicarrier Systems", in Signal Process., *IEEE Trans. on* , vol.60, no.7, July 2012.

[12] Wang, X.; Wild, T.; Schaich, F.; Brink, S.T., "Pilot-Aided Channel Estimation for Universal Filtered Multi-Carrier," *VT Conf.*, 2015.

[13] Boyd, S.; et al., "Convex optimization", *Cambridge Univ. Press*, 2004.

[14] LTE E-UTRA; Requirements for support of radio resource management (3GPP TS 36.133 version 12.10.0 Release 12).

[15] Extended vehicular A (EVA) channel. Available: http://www.raymaps.com/index.php/lte-multipath-channel-models.

[16] IEEE 802.16m Evaluation Methodology Document (EMD), "IEEE 802.16m-08/004r2", pp. 143, July 2008.

[17] Stupia, I.; Giannetti, F.; Lottici, V.; Andreotti, R.; Vandendorpe, L.; D'Andrea, A.N., "A greedy algorithm for goodput-oriented AMC in turbo-coded OFDM," *in Future Network and Mobile Summit*, 2010.